Peripheral neuroectodermal tumour of the kidney (Ewing's sarcoma): Restaging with ^{18}F-fluorodeoxyglucose (FDG)-PET/CT

Hakan Ozturk, MD

Department of Urology, School of Medicine, Sifa University, Izmir-Turkey

Cite as: *Can Urol Assoc J* 2015;9(1-2):E39-44. http://dx.doi.org/10.5489/cuaj.2286
Published online January 12, 2015.

Abstract

Primitive peripheral neuroectodermal tumour and Ewing's sarcoma (PNET/EWS) were originally described as two distinct pathologic entities, although both share common stem-cell precursor and unique chromosomal abnormality. Although its incidence has increased recently, its share in all sarcomas is 1%. It is usually seen in men and women in their twenties. We present a case of a 38-year-old woman with a left renal mass detected incidentally. Magnetic resonance imaging revealed a centrally located hypervascular renal mass with diameter of 6 cm with non-homogenous contrast enhancement containing necrotic and calcific areas. The patient was diagnosed as having PNET/EWS by histopathological examination following radical nephrectomy. Para-aortic lymph node metastasis was found on imaging by ^{18}F-fluorodeoxyglucose (FDG)-positron-emission tomography/computed tomography (PET/CT).

Introduction

Primitive neuroectodermal tumours/Ewing's sarcoma (PNET/EWS) is a rare disease first recognized by Arthur Purdy Stout in 1918 and classified within the family of small round cell tumours.[1] PNET/EWSs are more prevalent in children and occur more often in the central nervous system than in peripheral areas. Peripheral PNET is uncommon, accounting for only about 1% of all sarcomas.[2] The incidence of peripheral PNET/EWS in the abdomen and pelvis, including the retroperitoneum, is about 14% of all peripheral PNET/EWSs. It has rarely been described in the genitourinary system, including kidney, bladder, prostate, testis, ovary, and uterus.[2] The peak incidence of PNET/EWS is in adolescence and young adulthood, with most reported patients under 35.[3] Peripheral PNET/EWS arises outside the central and sympathetic nervous systems and differs from central PNET in that peripheral PNET/EWS typically expresses high amounts of the MIC2 antigen (CD99) and exhibits highly characteristic chromosomal translocation.[4] PNET/EWS is a very aggressive neoplasm and has a poor prognosis, with a 5-year disease-free survival rate of 45% to 55%.[5] In the present study, the patient's response to chemotherapy due to PNET/EWS was evaluated by ^{18}F-fluorodeoxyglucose (^{18}FDG)-PET/CT.

Case report

A 38-year-old female patient presented with a left renal mass with a diameter of 6 cm incidentally detected on ultrasonography. The physical examination revealed normal findings and we tallied the patient's biochemical analyses (Table 1). The patient was a nonsmoker. The magnetic resonance imaging (MRI) showed a solid primary kidney carcinoma in the left kidney with a central location, measuring 60 × 58 × 60 mm with a hypointense appearance in T1A, and a hyperintense appearance and intense contrast uptake in T2A sequences. Areas of calcification and necrosis were observed in the mass (Fig. 1). The patient underwent transperitoneal radical nephrectomy.

In the specimen taken after the left radical nephrectomy, the tumour mass with yellow-brown surface was 60 × 50 × 55 mm in size, located centrally, surrounded by the renal capsule, and showed foci of hemorrhage and necrosis. The microscopic examination revealed a tumour composed of monotonous round cells with hyperchromatic round nucleus. The interspersed small dark cells indicating pyknosis of the tumor cells could form rosette-like structures. The tumour cells were positive for CD99, S-100, vimentin and neuron-specific enolase (NSE). The tumour was desmin, synaptophysin, chromogranin negative (Fig. 2).

^{18}F-fluorodeoxyglucose (FDG)-positron-emission tomography/computed tomography (PET/CT) examination of the patient revealed a left para-aortic lymph node metastasis with diameter of 17 mm and standard uptake value (SUV_{max}) of 7.2 (Fig. 3, Table 2). The patient was started on iphosphamide + etoposide-based chemotherapy upon the diagnosis of PNET/EWS. Based on European Organisation for Research

Table 1. Biochemical analyses

Test	Results
Glucose	101 mg/dL
Creatinine	0.6 mg/dL
Urea	35 mg/dL
Aspartate aminotransferase	Normal
Alanine aminotransferase	Normal
Alkaline phosphatase	Normal
Gamma glutamyl transferase	Normal
White blood cells	5.22 × 10^3/μL
Hemoglobin	14.1 g/dL
Sodium	134 mmol/L
Potassium	4.2 mmol/L
Chloride	99 mEq/L
Calcium	9.3 mg/dL

and Treatment of Cancer (EORTC) criteria, partial remission was achieved by first-line chemotherapy. The cycles of therapy courses were administered every 21 days for 17 courses. Metastatic lymph node on the ^{18}FDG-PET/CT after first-line chemotherapy was 14 mm in size, with a SUV_{max} of 4.6 (Fig. 4). Complete remission was achieved by second-line chemotherapy (Fig. 5). The length of progression-free survival was 24 months and no metastasis or recurrence was found at the 72-month follow-up.

Discussion

PNET/EWS is a member of the family of primitive neuroectodermal tumours; these tumours most frequently occur in the paraspinal region and the thoracic wall. Renal origin is extremely rare, although cases reported with renal origin has increased recently. The first known case of PNET/EWS with renal origin was reported in 1975.[6] The tumour may occur at age of 5 or 6, but 75% of patients are between 10 and 39. The mean age is 26 and the tumour occurs most often in women.[7] Although its mechanism of development is not known, it is similar to that of neuroblastomas and it is believed that it is differentiated from tumours that are derivative of the neural crest. The less widely accepted view is that it originates from mesenchymal stem cells.[8]

As with all tumours of mesenchymal origin, PNET/EWSs do not lead to symptoms before reaching a larger size. These tumours usually have a pseudo-capsule, which is surgically unreliable and usually has been infiltrated by the tumour. For the cases reported in the literature, tumour size ranges between 5.5 and 23 cm.[9] In the literature, PNET/EWS has been reported to cause thrombus of the tumour in the renal vein, vena cava inferior, and right heart.[10,11] The clinical findings are uncharacteristic and patients usually complain of pain (85%), palpable masses (60%), and hematuria (37%).[12] No specific signs of PNET/EWS have been described in ultrasonography, CT, or MRI. Using ultrasonography, the tumour appears isoechogenic or hyperechogenic to the renal parenchyma. CT findings include areas of internal hemorrhage or necrosis, peripheral hypervascularity, and diffuse calcification. On MRI, the tumour appears isointense or hypointense on T1-weighted images, but heterogeneous on intermediate to high T2 signal intensity.[13]

The differential diagnoses include Wilm's tumour, neuroblastoma, renal cell carcinoma (RCC), malignant lymphoma, metastatic renal involvement from sarcoma elsewhere in the body, and renal involvement by a primary retroperitoneal sarcoma.[9,13] The pathological pictures leading to a diagnosis of PNET/EWS are the presence of neurosecretory granules with electron microscopy and the presence of rosettes or pseudorosettes with light microscopy.[8] NSE, chromogranin A, synaptophysin CD56, CD3, CD20, CD99, CD117, WT-1, Fli-1, AE1/AE3, MYF-4, desmin, S-100 and TdT are used in immunohistochemical examination, but the expression of surface antigen CD99 is diagnostic. The cloning of the breakpoints of the specific chromosomal translocations t (11; 22)(q24; q12) (EWS-FLI1 (85%) and t (21; 22)(q22; q12) EWS-ERF (10-15%) that are present in about 90% of PNET/EWSs permits the use of the reverse transcription polymerase chain reaction (RT-PCR) to detect specific fusion transcripts in these tumours. Other EWS fusions occur rarely (ETV1, E1AF, FEV). Transcription of

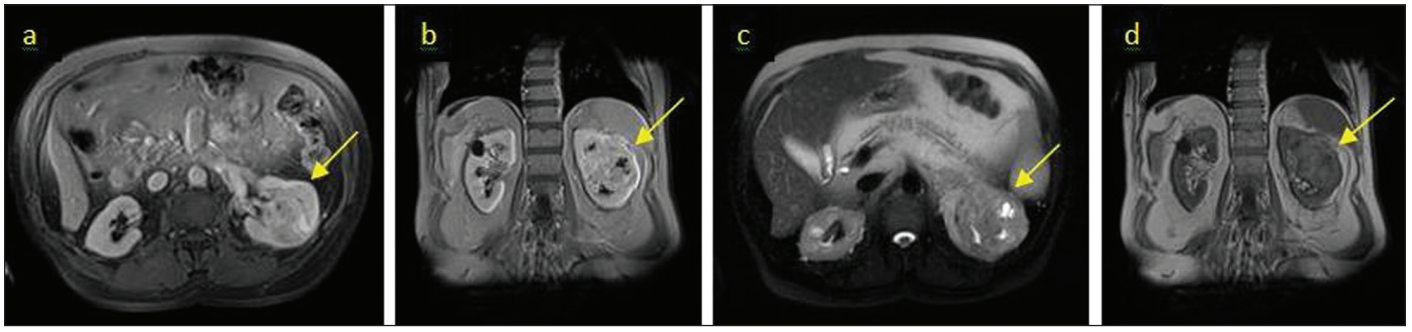

Fig. 1. A: Magnetic resonance imaging (MRI) T2, mass in the central part of the left kidney with necrosis (yellow arrow); B: MRI T2, mass in the central part of the left kidney with necrosis and calcification (yellow arrow); C: MRI T1 shows a mass in the central part of the left kidney with necrosis and calcification (yellow arrow); D: MRI T1 showing a mass in the central part of the left kidney with necrosis (yellow arrow).

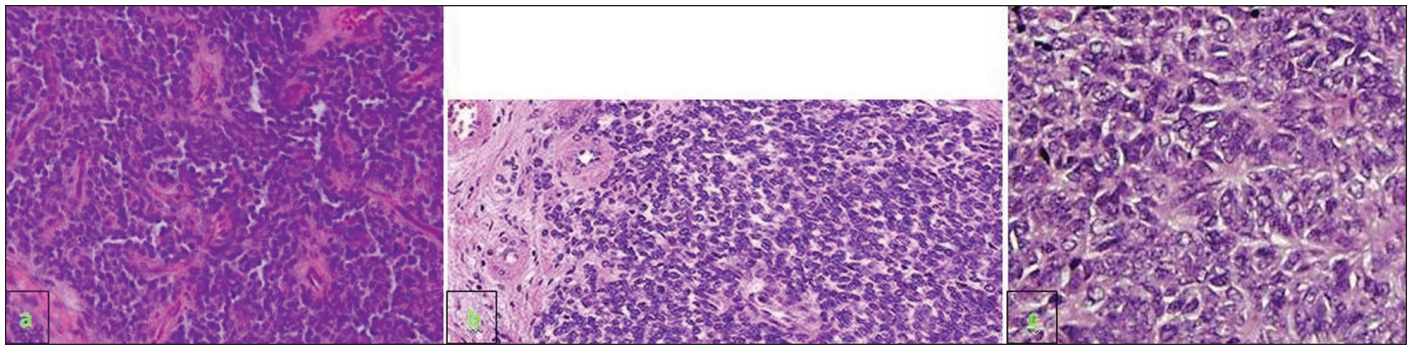

Fig. 2. Immunohistochemical examination. A: Small round cells for typical primitive peripheral neuroectodermal tumour and Ewing's sarcoma, as per hematoxylin & eosin staining (×200). B: Peripheral primitive neuroectodermal tumour with Homer Wright rosettes. The rosettes contain a circular wreath of oval nuclei that surround a pale eosinophilic, fibrillary core; C: Rosette formation. Positive immunoreactivity for CD99.

EWS-FLi and EWS-ERF may be confirmed by molecular analysis using PCR (Fig. 6, Table 3).

PNET/EWSs are aggressive and characterized by early metastatic disease (25%–50% at presentation); they are considered a systemic disease. Patients undergoing only local therapy have a recurrence rate of 80% to 90%, presumably because of subclinical metastasis at the time of the initial diagnosis.[14] In addition to local lymph node involvement, renal PNET/EWS often metastasizes to the lung, liver, and bone.[9,13] The MRI and CT can accurately assess local resectability and detect distant metastases. Bone scanning using 99-technetium has been recommended to detect bone metastases. Our patient had systemic disease and started chemotherapy due to para-aortic lymph node metastasis. As with all malignancies, the major problem for PNET/EWS is the inability to detect occult metastases with a high sensitivity using conventional methods. Conventional methods (e.g., ultrasound, CT, and MRI) can accurately diagnosis metastasis 70% of the time. Bone scanning with 99-technetium has the same limitation. It is well-known that metastases may occur in normal-appearing tissues and lymph nodes. Detecting metastases in the tissues infiltrated by high-activity tumour cells without any anatomic alteration is possible only with PET/CT, in which anatomic and functional images are combined. False-negative rates may be reduced by obtaining functional images. Indeed, in the present case, para-aortic lymph node metastasis was not detected by CT, but recognized by PET/CT. Response to chemotherapy was evaluated and the decision to proceed to second-line chemotherapy was made based on PET/CT findings.

Patients with localized tumour have a 5-year disease-free survival rate of about 45% to 55%. Despite aggressive treatment, the prognosis of patients with metastatic disease is poor, with overall cure rate of 20%. One of the main

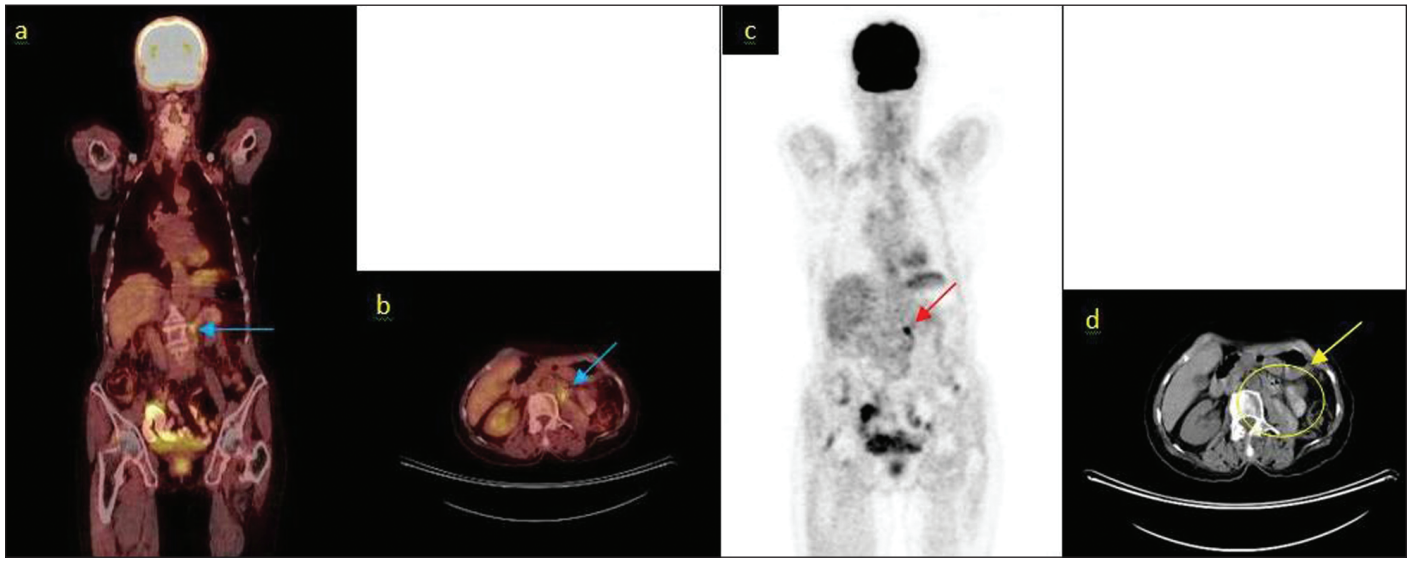

Fig. 3. Positron-emission tomography/computed tomography (PET/CT) images of the patient before chemotherapy; A: Revelations from the coronal ^{18}FDG-PET/CT scans (arrow: para-aortic lymph node metastasis), standard uptake value (SUV_{max}) 7.2; B: Revelations from the axial ^{18}FDG-PET/CT scans (arrow: para-aortic lymph node metastasis), SUV_{max} 7.2. C: Revelations from the maximum intensity projection images (arrow: para-aortic lymph node metastasis); D: Revelations from the axial CT scans (undedectable para-aortic lymph node metastasis).

Table 2. Evaluation of response of the patient to treatment by PET/CT based on EORTC criteria

	Metastatic foci	Size(mm)	SUVmax	EORTC Criteria
Pre-CTx	Para-aortic lymph node	17	7.2	Metastatic disease
First-line CTx	Para-aortic lymph node	14	4.6	Partial remission
Second-line CTx	Any metastatic foci	0	0	Completed remission

CTx: chemotheraphy; SUV: standard uptake value; EORTC: European Organisation for Research and Treatment of Cancer.

challenges is proper diagnosis and adequate expedient treatment.[12,15,16] In their analysis of 7 patients with renal EWS and with median follow-up of 36 months (range: 5–149), Mukkunda and colleagues found a median disease-free survival in patients with non-metastatic disease of 30.35 months (range: 5.1–149) with a 5-year overall survival rate of 42%.[17] All PNETs show a 5-year survival rate of 58% to 61%, with a median survival of 120 months.[18] In comparison, in their analysis of adult patients with localized Ewing's sarcoma in bone and soft tissue, Gupta and colleagues found a 3-year event-free survival rate of 43% ± 13%.[19]

The most important step in the treatment of the disease is radical nephrectomy involving lymph node dissection. Radiation therapy may be used only for positive margins or for the tumours extending beyond the Gerota's fascia. Even though the disease is treated in local stages, chemotherapy is usually inevitable because of occult micrometastases with high recurrence rates and aggressive potential of the tumour. According to International Ewing's Sarcoma Study (IESS)-1 and IESS-2, the chemotherapy regimen consisting of vincristine (V), doxorubicin (A), cyclophosphamide (C), actinomycin (A) (VDCA protocol) was recommended. In the IESS-3 study, it was reported that adding iphosphamide (I) and etoposid (E) to the VDCA regimen increased the 5-year disease-free survival (54% vs. 69%).[20] In our patient, alternant first- and second-line chemotherapy protocols were used based on IESS-criteria. Complete response to chemotherapy was achieved. At the 72-month follow-up, the patient was recurrence-free.

In the literature, sensitivity of 63% to 88% and specificity of 75% to 100% have been reported for ^{18}FDG-PET/CT in detecting recurrences and metastatic disease in renal tumours.[21] Findings are similar for the variant tumours of the kidney. The most distinctive feature of the cancer tissue is that it shows higher glucose metabolism than normal tissues (Warburg effect).[22] Since PNET/EWSs are aggressive tumours with high metastatic potential, their Warburg effect, their SUV, is high due to high glucose metabolism. Thus, they are more easily recognized on the PET/CT detector. Wu and colleagues have compared ^{18}F-FDG PET and technetium-99m methylene diphosphonate bone scans documenting higher sensitivity and accuracy of positron imaging in detecting bone metastases in patients affected by RCC.[23] Franzius and colleagues compared PET and bone scans using 99-technetium in their study of 38 patients, in which sensitivity of the bone metastases were determined in patients with PNET/EWS. Sensitivity, specificity, and accuracy rates were 100%, 96%, and 97%, respectively, for PET whereas 68%, 87%, and 82% for bone scans.[24]

Daldrup and colleagues evaluated bone metastases by MRI in PNET/EWS and compared the findings with those of PET. Sensitivity was 80% and 85%, for MRI and PET, respectively.[25] Györke and colleagues found sensitivity of 96% and specificity of 78% for PET examination in 13 patients with PNET/EWS.[26] In a 2010 study, Mody and colleagues found a sensitivity of 87% and specificity of 83% for PET.[27] Vrachimis and colleagues found that PET and PET/CT were superior to conventional methods in staging and detecting recurrence in PNET/EWS. PET/CT may detect occult metastases and alter treatment decision in some cases.[28] In their meta-analysis, Treglia and colleagues found that PET/CT was more sensitive and more specific than PET for PNET/EWS (Table 4).[29]

The technical problems of PET/CT should be recognized. In the studies conducted so far, tumours can be detected by PET/CT imaging only in the presence of tumour cells at a certain number (10^4–10^7) having abnormal and increased glucose metabolism. Such diagnostic failures are more common, especially in lung and liver metastases. Lung metastases under 5 mm cannot be evaluated accurately; the reason

Table 3. Clinical, radiologic, pathologic, genetic features of PNET/EWS

	Clinical features	Radiologic features	Pathologic features	Genetic features
PNET/EWS	• Flank pain • Hematuria • Abdominal mass • Weight loss	• Large size • Lack of extensive parenchyma infiltration • Lack of renal vein invasion • Diffuse large calcification • Internal hemorrhage and necrosis • Peripheral hypervascularity	• Presence of neurosecretory granules • Presence of rosettes (electron microscopy) or pseudorosettes (light microscopy) • Neuron-specific enolase • Chromogranin A • Synaptophysin	• Glycoprotein p30/32 (monoclonal antibody) CD99 (encoded by the MIC2 gene) • Specific chromosomal translocations t (11; 22) (q24; q12); t (21; 22) (q22; q12) EWSR1 gene rearrangement

PNET/EWS: Primitive peripheral neuroectodermal tumour and Ewing's sarcoma.

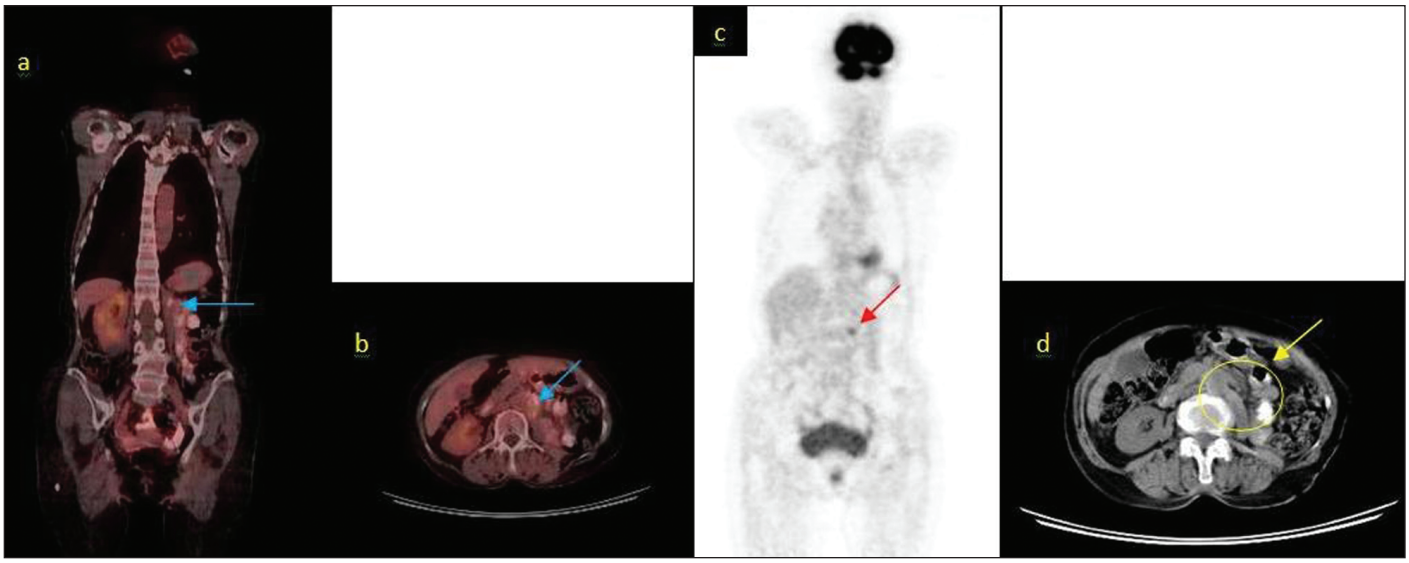

Fig. 4. Positron-emission tomography/computed tomography (PET/CT) images of the patient after first-line chemotherapy. A: Revelations from the coronal ^{18}FDG-PET/CT scans (arrow: para-aortic lymph node metastasis), standard uptake value (SUV_{max}) 4.6; B: Revelations from the axial ^{18}FDG-PET/CT scans (arrow: para-aortic lymph node metastasis), SUV_{max} 4.6; C: Revelations from the maximum intensity projection images (arrow: para-aortic lymph node metastasis); D: Revelations from the axial CT scans (undedectable para-aortic lymph node metastasis).

for this is unknown. It is believed that it may be due to either movement artifact of the lungs or lower metabolic activity of the metastatic mass. Minimizing movement artifacts and obtaining improved spatial resolution may increase the diagnostic accuracy for these lesions.[30]

Conclusion

Disease-specific survival is poor in PNET/EWS due to its aggressive and unknown biological behaviour. It is still unclear whether genetics play a role. The inability to detect micrometastases and protocols for follow-up and response to the treatment are still important problems. The ^{18}FDG-PET/CT protocol has been proposed as the standard in diagnosing the occult micrometastases and metastatic disease, and in evaluating response to the chemotherapy.

Competing interests: Authors declare no competing financial or personal interests.

This paper has been peer-reviewed.

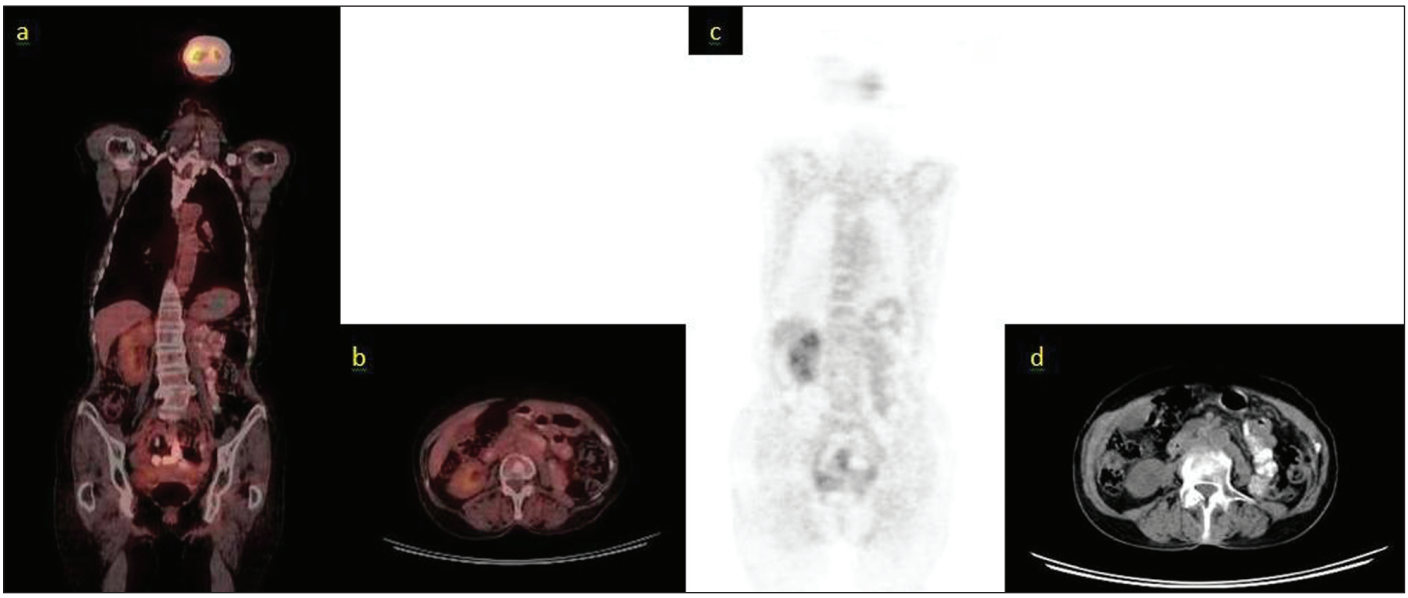

Fig. 5. Normal positron-emission tomography/computed tomography of the patient with complete remission following second-line chemotherapy.

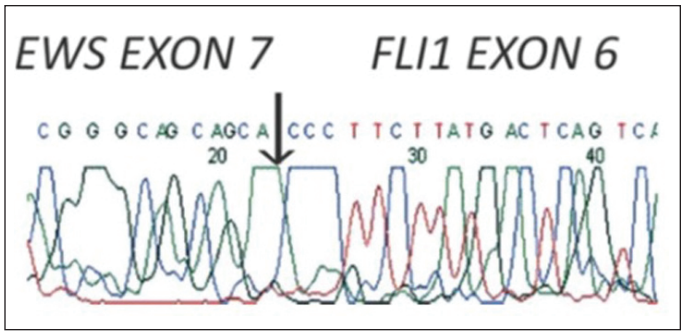

Fig. 6. Genetic defect of Ewing's sarcoma (EWS-FLi).

Table 4. Diagnostic performance of PET/CT studies in the literature

Author	Modality	n	Sensitivity (%)	Specificity (%)
Györke et al.[26]	FDG-PET	13	96	78
Mody et al.[27]	FDG-PET	5	87	83
Vrachimis et al.[28]	FDG-PET/CT	7	NA	NA
Treglia et al.[29]	PET/CT(PET)		96(95)	95(92)

PET/CT: positron-emission tomography/computed tomography; FDG: 18F-fluorodeoxyglucose.

References

1. Pomara G, Cappello F, Cuttano MG, et al. Primitive neuroectodermal tumor of the kidney: A case report. *BMC Cancer* 2004;4:3. http://dx.doi.org/10.1186/1471-2407-4-3
2. Kim MS, Kim B, Park CS, et al. Radiologic findings of peripheral primitive neuroectodermal tumor arising in the retroperitoneum. *AJR Am J Roentgenol* 2006;186:1125-32. http://dx.doi.org/10.2214/AJR.04.1688
3. Llombart-Bosch A. Ewing's sarcoma and peripheral primitive neuroectodermal tumor of bone and soft tissue. *Int J Surg Pathol* 1999;7:185-92. http://dx.doi.org/10.1177/106689699900700401
4. Dedeurwaerdere F, Giannini C, Sciot R, et al. Primary peripheral PNET/Ewings's sarcoma of the dura: A clinicopathologic entity distinct from central PNET. *Mod Pathol* 2002;15:673-8. http://dx.doi.org/10.1038/modpathol.3880585
5. Jurgens H, Bier V, Harms D, et al. Malignant peripheral neuroectodermal tumors: A retrospective analysis of 42 patients. *Cancer* 1988;61:349-57. http://dx.doi.org/10.1002/1097-0142(19880115)61:2<349::AID-CNCR2820610226>3.0.CO;2-0
6. Seemayer TA, Thelmo WL, Bolande RP, et al. Peripheral neuroectodermal tumors. *Perspect Pediatr Pathol* 1975;2:151-72.
7. Jimenez RE, Folpe AL, Lapham RL, et al. Primary Ewing's sarcoma/primitive neuroectodermal tumor of the kidney: A clinicopathologic and immunohistochemical analysis of 11 cases. *Am J Surg Pathol* 2002;26:320-7. http://dx.doi.org/10.1097/00000478-200203000-00005
8. Quezado M, Benjamin DR, Tsokos M. EWS/FLI-1 fusion transcripts in three peripheral primitive neuroectodermal tumors of the kidney. *Hum Pathol* 1997;28:767-71. http://dx.doi.org/10.1016/S0046-8177(97)90147-7
9. Lalwani N, Prasad SR, Vikram R, et al. Pediatric and adult primary sarcomas of the kidney: A cross-sectional imaging review. *Acta Radiologica* 2011;52:448-57. http://dx.doi.org/10.1258/ar.2011.100376
10. Fergany AF, Dhar N, Budd GT, et al. Primary extraosseous ewing sarcoma of the kidney with level III inferior vena cava thrombus. *Clin Genitourin Cancer* 2009;7:E95-7. http://dx.doi.org/10.3816/CGC.2009.n.032
11. Rizzo D, Barone G, Ruggiero A, et al. Massive venous thrombosis of inferior vena cava as primary manifestation of renal Ewing's sarcoma. *Clin Nephrol* 2011;75:560-4. http://dx.doi.org/10.5414/CN106555
12. Angel JR, Alfred A, Sakhuja A, et al. Ewing's sarcoma of the kidney. *Int J Clin Oncol* 2010;15:314-8. http://dx.doi.org/10.1007/s10147-010-0042-0
13. Ellinger J, Bastian PJ, Hauser S, et al. Primitive neuroectodermal tumor: Rare, highly aggressive differential diagnosis in urologic malignancies. *Urology* 2006;68:257-62. http://dx.doi.org/10.1016/j.urology.2006.02.037
14. Ekram T, Elsayes KM, Cohan RH, et al. Computed tomography and magnetic resonance features of renal ewing sarcoma. *Acta Radiologica* 2008;49:1085-90. http://dx.doi.org/10.1080/02841850802345618
15. Wedde TB, Lobmaier IVK, Brennhovd B, et al. Primary ewings sarcoma of the kidney in a 73-year-old man. *Sarcoma* 2011;2011:978319.
16. Risi E, Iacovelli R, Altavilla A. Clinical and pathological features of primary neuroectodermal tumor/Ewing sarcoma of the kidney. *Urology* 2013;82:382-6. http://dx.doi.org/10.1016/j.urology.2013.04.015
17. Mukkunda R, Venkitaraman R, Thway K, et al. Primary adult renal Ewing's Sarcoma: A rare entity. *Sarcoma* 2009;504654. http://dx.doi.org/10.1155/2009/504654
18. Mani S, Dutta D, de Binay K. Primitive neuroectodermal tumor of the liver: A case report. *Japan J Clin Oncol* 2009;40:258-62. http://dx.doi.org/10.1093/jjco/hyp158
19. Gupta A, Pappo A, Saunders N, et al. Clinical outcome of children and adults with localized Ewing sarcoma: Impact of chemotherapy dose and timing of local therapy. *Cancer* 2010;116:3189-94. http://dx.doi.org/10.1002/cncr.25144
20. Brasme JF, Chalumeau M, Oberlin O, et al. Time to diagnosis of ewing tumors in children and adolescents is not associated with metastasis or survival: A prospective multicenter study of 436 patients. *J Clin Oncol* 2014;32:1935-40. http://dx.doi.org/10.1200/JCO.2013.53.8058
21. Rodrýguez Martý nez de Llano S, Jime nez-Vicioso A, Mahmood S, et al. Clinical impact of (18)F-FDG PET in management of patients with renal cell carcinoma. *Rev Esp Med Nucl* 2010;29:12-9. http://dx.doi.org/10.1016/j.remn.2009.11.008
22. Gillies RJ, Robey I, Gatenby RA. Causes and consequences of increased glucose metabolism of cancers. *J Nucl Med* 2008;49:24S-42S. http://dx.doi.org/10.2967/jnumed.107.047258
23. Wu HC, Yen RF, Shen YY, et al. Comparing whole body 18F-2-deoxyglucose positron emission tomography and technetium-99m methylene diphosphate bone scan to detect bone metastases in patients with renal cell carcinomas: A preliminary report. *J Cancer Res Clin Oncol* 2002;128:503-6. http://dx.doi.org/10.1007/s00432-002-0370-1
24. Franzius C, Sciuk J, Daldrup-Link HE, et al. FDG-PET for detection of osseous metastases from malignant primary bone tumours: Comparison with bone scintigraphy. *Eur J Nucl Med* 2000;27:1305-11. http://dx.doi.org/10.1007/s002590000301
25. Daldrup-Link HE, Franzius C, Link TM, et al. Whole-body MR imaging for detection of bone metastases in children and young adults: Comparison with skeletal scintigraphy and FDG PET. *AJR Am J Roentgenol* 2001;177:229-36. http://dx.doi.org/10.2214/ajr.177.1.1770229
26. Györke T, Zajic T, Lange A, et al. Impact of FDG PET for staging of Ewing sarcomas and primitive neuroectodermal tumours. *Nucl Med Commun* 2006;27:17-24. http://dx.doi.org/10.1097/01.mnm.0000186608.12895.69
27. Mody RJ, Bui C, Hutchinson RJ, et al. FDG PET imaging of childhood sarcomas. *Pediatr Blood Cancer* 2010;54:222-7.
28. Vrachimis A, Dirksen U, Wessling J, et al. PET surveillance of patients with Ewing sarcomas of the trunk: Must the lower legs be included? *Nuklearmedizin* 2010;49:183-6. http://dx.doi.org/10.3413/nukmed-03131004
29. Treglia G, Salsano M, Stefanelli A, et al. Diagnostic accuracy of ^{18}F-FDG-PET and PET/CT in patients with Ewing sarcoma family tumours: A systematic review and a meta-analysis. *Skeletal Radiol* 2012;41:249-56. http://dx.doi.org/10.1007/s00256-011-1298-9
30. El Fakhri G, Surti S, Trott CM, et al. Improvement in lesion detection with whole-body oncologic time-of-flight PET. *J Nucl Med* 2011;52:347-53. http://dx.doi.org/10.2967/jnumed.110.080382

Correspondence: Dr. Hakan Ozturk, Basmane Hospital of Sifa University, Fevzipasa Boulevard No: 172/2, 35240, Basmane-Konak-Izmir/Turkey; drhakanozturk@yahoo.com.tr